Technical Note

Analysis and Correction of the Seafloor Topography Distortion Caused by the Sound Velocity Error for MBS Soundings

Wenzhou Sun [1,2,*], Anmin Zeng [1] and Xiang Zhao [2]

[1] *State Key Laboratory of Geo-Information Engineering, Xi'an 727500, China*

[2] *Xi'an Research Institute of Surveying and Mapping, Xi'an 727500, China*

* Correspondence: wenzhou_sun@163.com; Tel.: +86-059-26325520

Abstract: We found an important fact that the beam footprint line of *Ping* will intersect with the real water depth when the initial incidence angle is about 45°, and sound velocity error hardly has an effect on it. This is contrary to our previous experience that the soundings of the central beam of multi-beam bathymetric system (MBS) is the most accurate. Firstly, the influence of sound velocity errors on central beam and seafloor topography distortion was analyzed. Secondly, the process of proving this fact was given, and the topography correction method was proposed by compensating the sound velocity profile area (SVP area). Finally, we showed in the first simulation of four type errors in SVPs that this fact is verified. The topography correction method used in the second simulation to correct the topography distortion of the first simulation is also verified.

Keywords: multi-beam bathymetric system (MBS); seafloor topography distortion; SVP area; acoustic ray tracing; beam footprint.

1. Introduction

Muti-beam bathymetric system (MBS) is frequently used for marine depth measurement. In the process of MBS soundings, one of the key steps is sound velocity correction. To reduce the influence of sound velocity errors on soundings, two groups of sound velocity profiles (SVP) shall be measured with CTD (Conductance, Temperature, Depth) before and after the MBS carries out, respectively. Then, the SVP is selected by the time and space proximity principle for calculating the beam footprints based on the acoustic ray tracing method. However, there are errors between the measured SVP and the real SVP due to the physical mechanism of CTD and complex ocean phenomena[1,2], which leads to the topography distortion for MBS soundings [3].

It is generally accepted that the central beam of MBS has the smallest sounding errors, and as the initial incidence angle increases, the sounding errors also increase [4]. The coefficient method is a popular technique to correct the deviation data of MBS soundings, which calculates the error coefficient between the survey soundings and the actual soundings in a flat sea area. Then, the error coefficient is used to correct the soundings of other sea areas[5,6]. Xiao proposed to construct a submarine topography trend line with adjacent central beams as prior information[7]. Then, Kalman Filter (KF) is applied to correct the systematic errors of soundings caused by sound velocity errors. Zhao also put forward an opinion that the footprint of the marginal beams upwarps due to the SVP errors, while the central beam is less affected by it, which can correctly reflect the actual seafloor topography change[8]. Wu also believes that the errors of marginal beams mainly influence the quality of multi-beam soundings, and the key factor of marginal beam quality is accurate SVP[9].

All the above studies for correcting distorted topography are based on the viewpoint of the soundings of the central beam is the most accurate. However, this paper presents a critical conclusion that the beam footprint is closest to the real seafloor when the initial incidence angle is about 45 °. This conclusion is proven theoretically and experimentally in the following section. In

Preprints (www.preprints.org) | NOT PEER-REVIEWED | Posted: 28 April 2023 doi:10.20944/preprints202304.1156.v1

Sect.2.1, two types of ray tracing methods are introduced. In Sect.2.2, the influence of sound velocity errors on the soundings of the central beam is analyzed. In Sect.2.3, the topography distortion law caused by sound velocity errors is studied. In Sect. 2.4, we proved an important fact that the sounding errors are the smallest when the beam angle is about 45° instead of the central beam. In Sect. 3.1, a simulation is launched to verify our theoretical analysis. In Sect. 3.2, a method is proposed to correct the topography distortion by compensating the sound velocity profile area, and another simulation is carried out to correct the distorted topography data shown in the first simulation.

2. Materials and Methods

2.1 Ray tracing method

The ray tracing method is generally used for searching the position of beam footprints because of its high accuracy. There are two types of calculation processes for this method. One assumes that the sound velocity gradient of the unit water layer is a constant (the Constant Gradient Ray Tracing Method, CGRT). The other assumes that the sound velocity gradient of the unit water layer is zero (the Zero Gradient Ray Tracing Method, ZGRT). The CGRT method has higher accuracy because its assumption is closer to the real sound velocity profile, However, it also brings greater computational complexity. The accuracy of the two methods is relatively close when the stratified interval of water layers is quite small. To make the proof more feasible to proceed, the ZGRT method is used for the following derivation process[10,11] . Figure 1 shows the acoustic ray trajectory of the ZGRT method.

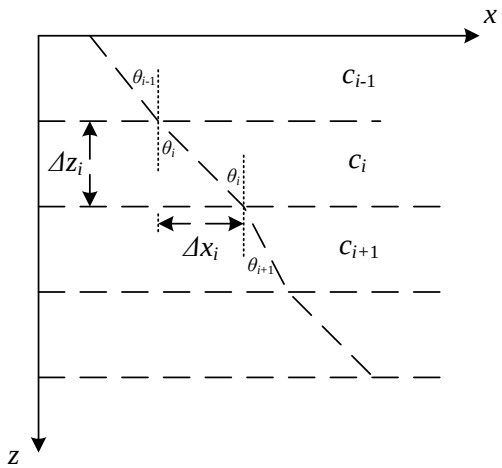

Figure 1. The acoustic ray trajectory of the zero gradient ray tracing method.

If the acoustic ray propagates with a constant sound velocity (zero gradients) in unit water layer i, the horizontal distance Δx_i and the propagation time Δt_i can be expressed as [12,13]

$$\Delta x_i = \Delta z_i \cdot \tan\theta_i = \frac{\sin\theta_i \cdot \Delta z_i}{\cos\theta_i} = \frac{p \cdot c_i \cdot \Delta z_i}{\left(1-(pc_i)^2\right)^{1/2}} \quad (1)$$

$$\Delta t_i = \frac{\Delta x_i / \sin\theta_i}{c_i} = \frac{\Delta x_i}{p \cdot c_i^2} = \frac{\Delta z_i}{c_i \cdot \left(1-(pc_i)^2\right)^{1/2}} \quad (2)$$

Where p is Snell's refraction constant, c_i, θ_i, and Δz_i are the sound velocity, the beam incidence angle, and the thickness of the water layer i, respectively.

In the process of acoustic ray tracing, Δx_i and Δt_i are calculated layer by layer and accumulated as $\Sigma\Delta x_i$ and $\Sigma\Delta t_i$. This process ends when the $\Sigma\Delta t_i$ reaches the observation time t measured by MBS.

Preprints (www.preprints.org) | NOT PEER-REVIEWED | Posted: 28 April 2023 doi:10.20944/preprints202304.1156.v1

The horizontal displacement and the vertical displacement in the last water layer are respectively[14]

$$\Delta x_n = dt \cdot c_n \cdot \sin\theta_n \quad (3)$$

$$\Delta z_n = dt \cdot c_n \cdot \cos\theta_n \quad (4)$$

Where, $dt = T - \sum_{i=1}^{n-1} \Delta t_i$, is the residual time of acoustic ray tracing, c_n, and θ_n are the sound velocity and the incident angle in the last water layer, respectively. The positions of the beam footprint are obtained by accumulative the horizontal displacement Δx_i and vertical displacement Δz_i of the whole water layers.

2.2 Influence of sound velocity errors on the central beam

It is widely believed that the sounding accuracy of the central beam is higher than the marginal beams because the incident angle of the central beam in all the water layers is zero, and the acoustic ray does not bend during propagation. However, the sounding errors will still accumulate due to the inaccurate measurement of the sound velocity profile. The position of the central beam footprint will deviate from the actual seafloor depth in the vertical direction.

Since the incident angle of the acoustic ray is 0, the propagation time Δt_i of the central beam in the water layer i can be written as[15]

$$\Delta t_i = \frac{\Delta z_i}{c_i} = \frac{\Delta z_i^2}{\Delta s_i} \quad (5)$$

Where $\Delta s_i = c_i \times \Delta z_i$, is the area enclosed by the sound velocity profile and the z-axis in water layer i [16].

If the Δc_i is the measurement error of sound velocity c_i in water layer i, there would be an error δt_i with respect to the propagation time Δt_i and an error δs_i with respect to the SVP area Δs_i. Taking the sound velocity error Δc_i into account. Equation (5) can be rewritten as

$$\Delta s_i \cdot \Delta t_i + \Delta s_i \cdot \delta t_i + \delta s_i \cdot \Delta t_i + \delta s_i \cdot \delta t_i = \Delta z_i^2 \quad (6)$$

Since the δt_i and δs_i are less than a few parts in 10^3 of Δs_i and Δt_i, respectively. The second-order term $\delta t_i \cdot \delta s_i$ is much smaller than the others and can be neglected. For the actual values of Δs_i and Δt_i satisfy equation (5), δt_i can be described as

$$\delta t_i = -\frac{\Delta c_i \cdot \Delta t_i}{c_i} = -\frac{\delta s_i}{c_i^2} \quad (7)$$

If the sound velocity of each layer is replaced by the harmonic average sound velocity c_h, that will cause the error to be less than a few parts in 10^4 of the total propagation time, and the variation of the total propagation time δT for the whole water layer can be simplified as

$$\delta T = \sum_{i=1}^{n} \delta t_i = -\frac{1}{c_h^2} \cdot \delta S \quad (8)$$

Where δS is the SVP area for the whole water layers.

Equation (8) reveals the relationship between the variation of the propagation time δT and the SVP area difference δS. As the δS is positive, the δT is negative. It means that the accumulated time which is calculated by the ray tracing method from the surface layer to the last layer is less than the measured propagation time. So, the ray tracing program continues to run until the accumulated propagation time reaches the measured propagation time. Resulting in the sounding of the central beam is greater than the actual water depth. Similarly, the δT is positive when the δS is negative, which indicates that the beam footprint does not reach the real seafloor when the accumulated propagation time is equal to the measured propagation time. This will cause the water depth measured by the central beam to be smaller than the real water depth.

Preprints (www.preprints.org) | NOT PEER-REVIEWED | Posted: 28 April 2023 doi:10.20944/preprints202304.1156.v1

2.3 Topography distortion law caused by sound velocity error

The sounding error caused by the same SVP error changes along with the initial incidence angles. This would distort the measured marine topography into a convex or concave shape.

The relationship between the propagation time Δt_i and the depth Δz_i in the water layer i can be described as

$$\Delta z_i = c_i \cdot \Delta t_i \cdot \cos\theta_i \tag{9}$$

If the measured sound velocity with an error Δc_i, i.e., $c_i' = c_i + \Delta c_i$, the vertical displacement $\Delta z_i'$ on the same propagation time Δt_i is given by

$$\Delta z_i' = c_i' \cdot \Delta t_i \cdot \cos\theta_i' \tag{10}$$

where is the updated incident angle as the sound velocity varies.

From Equations (9) and (10), the vertical displacement deviation δz_i in water layer i can be derived as

$$\delta z_i = \Delta z_i' - \Delta z_i = \Delta z_i \cdot \left(\frac{\Delta z_i'}{\Delta z_i} - 1 \right) = \Delta z_i \cdot \left(\frac{c_i' \cdot \cos\theta_i'}{c_i \cdot \cos\theta_i} - 1 \right) \tag{11}$$

According to Snell's law, it has

$$\sin\theta_i' / c_i' = \sin\theta_i / c_i = p$$

The Equation (11) can be rewritten as

$$\delta z_i = \Delta z_i \cdot \left(\frac{\sin\theta_i' \cos\theta_i'}{\sin\theta_i \cos\theta_i} - 1 \right) = \Delta z_i \cdot \left(\frac{\sin 2\theta_i'}{\sin 2\theta_i} - 1 \right) \tag{12}$$

As Equation (12) shows, the displacement deviation δz_i is negative when $0° \le \theta_i' \le \theta_i < 45°$ or $45° \le \theta_i \le \theta_i' < 90°$, and the δz_i is positive when $45° \le \theta_i' \le \theta_i < 90°$ or $0° \le \theta_i \le \theta_i' < 45°$. It implies that the soundings are smaller than the actual sea depth when $0° \le \theta_i' \le \theta_i < 45°$ or $45° \le \theta_i \le \theta_i' < 90°$, and the soundings are greater than the actual sea depth when $45° \le \theta_i' \le \theta_i < 90°$ or $0° \le \theta_i \le \theta_i' < 45°$.

The Equation (12) can be rewritten as

$$\delta z_i = \Delta z_i \cdot \left(\frac{c_i + \Delta c_i}{c_i} \right) \cdot \frac{\sqrt{1 - p^2 \cdot (c_i + \Delta c_i)^2}}{\sqrt{1 - p^2 c_i^2}} - \Delta z_i \tag{13}$$

To analyze the relationship between the vertical displacement deviation δz_i and the initial incidence angle, the c_i and Δc_i can be taken as a constant. The derivative of δz_i with p is given by

$$\delta z_i'(p) = \Delta z_i \cdot \left(\frac{c_i + \Delta c_i}{c_i} \right) \cdot \frac{\dfrac{-p \cdot (c_i + \Delta c_i)^2}{\sqrt{1 - p^2 \cdot (c_i + \Delta c_i)^2}} \cdot \sqrt{1 - p^2 c_i^2} + \dfrac{2 p c_i^2}{\sqrt{1 - p^2 c_i^2}} \cdot \sqrt{1 - p^2 \cdot (c_i + \Delta c_i)^2}}{1 - p^2 c_i^2} \tag{14}$$

where $p = \sin(\theta_0)/c_0$ is Snell constant, θ_0 and c_0 are the initial incidence angle and surface sound velocity, respectively. If $\Delta c_i < 0$, the displacement deviation δz_i would decrease with the initial incidence angle θ_0 increasing. On the contrary, if $\Delta c_i > 0$, the δz_i would increase with the initial incident angle θ0 increasing.

Considering the whole water layers, $\delta Z = \sum_{i=1}^{n} \delta z_i$. If the SVP area δS is less than zero, the central beam footprint would be above the real seafloor. This leads to the vertical δZ displacement deviation decreasing as the initial incidence angle increases, and the shape of the calculated seafloor topography shows a convex shape. On the contrary, the calculated seafloor topography would show a shape of concave when the SVP area δS is bigger than zero.

Preprints (www.preprints.org) | NOT PEER-REVIEWED | Posted: 28 April 2023 doi:10.20944/preprints202304.1156.v1

2.4. An important fact about the initial incidence angle is 45 degree

Different from the previous viewpoint of the central beam has the most accuracy. We present an important fact that MBS has a minimal sounding error instead of the central beam when the initial incidence angle is about 45°. In this section, this fact would be proved as follow.

The SVP area in water layer i is defined as

$$\Delta s_i = c_i \cdot \Delta z_i \tag{15}$$

Taking into Equation (2), the propagation time in water layer i can be expressed as

$$\Delta t_i = \frac{\Delta z_i}{\cos\theta_i \cdot c_i} = \frac{\Delta s_i}{\cos\theta_i \cdot c_i^2} = k(c_i) \cdot \Delta s_i \tag{16}$$

Where $k(c_i) = \dfrac{1}{\cos\theta_i \cdot c_i^2}$ and $\cos\theta_i = \sqrt{1 - c_i^2 \cdot p^2}$.

Taking the partial derivative of Eq（16）with respect to c_i is given by

$$\begin{aligned} \frac{\partial \Delta t_i}{\partial c_i} &= \frac{\partial k(c_i)}{\partial c_i} \cdot \Delta s_i + \frac{\partial \Delta s_i}{\partial c_i} \cdot k(c_i) \\ &= \frac{-2 \cdot \Delta z_i}{c_i^2 \cdot \cos\theta_i} + \frac{p^2 \cdot \Delta z_i}{\cos^3\theta_i} + \frac{\Delta z_i}{c_i^2 \cdot \cos\theta_i} \\ &= \frac{-\Delta z_i}{c_i^2 \cdot \cos\theta_i} + \frac{p^2 \cdot \Delta z_i}{\cos^3\theta_i} \\ &= \Delta z_i \cdot p^2 \left(\frac{-1}{\sin^2\theta_i \cdot \cos\theta_i} + \frac{1}{\cos^3\theta_i} \right) \end{aligned} \tag{17}$$

The function $f(\theta)$ is defined as

$$f(\theta) = \frac{-1}{\sin^2\theta_i \cdot \cos\theta_i} + \frac{1}{\cos^3\theta_i} \tag{18}$$

Since the initial incidence angle θ_0 and layer thickness Δz_i is a constant, the $\Delta z_i \cdot p^2$ is a constant. The change law $\partial \Delta t_i / \partial c_i$ is only determined by the function $f(\theta)$. The greater the function $f(\theta)$ is, the more significant influence of the sound velocity disturbance on the propagation time. The smaller the function $f(\theta)$ is, the weaker influence of the sound velocity disturbance on the propagation time. The relationship between the function $f(\theta)$ and the incident angle is shown as Figure 2.

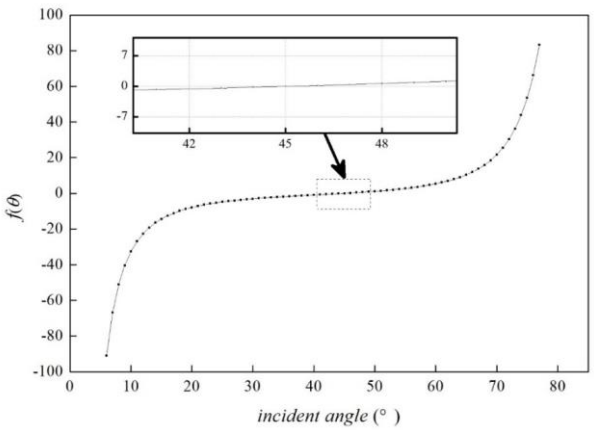

Figure 2. The function curve of $f(\theta)$.

Preprints (www.preprints.org) | NOT PEER-REVIEWED | Posted: 28 April 2023 doi:10.20944/preprints202304.1156.v1

It can be seen from Figure 2 that the function curve $f(\theta)$ is an approximate straight line and slowly increases when the incident angle varies from 20 ° to 60 °. The value of $f(\theta)$ is 0 when the incident angle is about 45°. It changes violently as the incident angle is smaller than 20 ° or bigger than 60 °.

The sound velocity has the vertical variation and the measurement error. Assuming that the initial incidence angle is 45°. The vertical variation range of sound velocity is range from -20m/s to 20m/s and the measurement error range of sound velocity is from -2m/s to 2m/s. The total variation of sound velocity will result in the fluctuation of the incident angle from 0.7589° to 0.7691. Equivalent to the vertical error is from 7.0687e-05 to 7.1637e-05 and the horizontal error is from 6.8838e-05 to 7.3586e-05 for the water depth is 1 m. It means that the influence of sound velocity error on the propagation time is relatively small when the initial incidence angle is about 45°. The measured depth obtained by the ray tracing method will be close to the real seafloor, and the horizontal displacement for the whole water layer is terribly small on the various SVP errors. Therefore, the beam footprint line affected by various SVP errors can be approximated regard as converging at the real water depth.

We draw the following conclusions through the previous theoretical analysis. 1) Soundings of the central beam are greater than the real water depth when the SVP area difference is positive, and it is less than the real water depth when the SVP area difference is negative. 2) The topography presents a concave shape when the SVP area difference is positive, and the topography presents a convex shape when the SVP area difference is negative. 3) The position of the beam footprint is near the real water depth for various sound velocity errors when the initial incidence angle is about 45°.

3. Simulated examples and analysis

3.1 Simulated examples

We carried out the following simulations to verify the above theoretical analysis. The SVP used in the simulations was obtained by the Munk standard equation[17]

$$C = C_1\left[1+\varepsilon\left(\eta+e^{-\eta}-1\right)\right] \tag{19a}$$

$$\eta = \left(z-z_1\right)/\frac{1}{2}B \tag{19b}$$

Where z_1=1000 m is the depth of the sound channel axis, C_1=1482 m/s is the sound velocity at this depth, ε=7.4×10^{-3} is the perturbation coefficient, B=1400 m is the stratification scale, and z is the depth to the sea surface. Figure 3 is a background SVP simulated by Eq. (19).

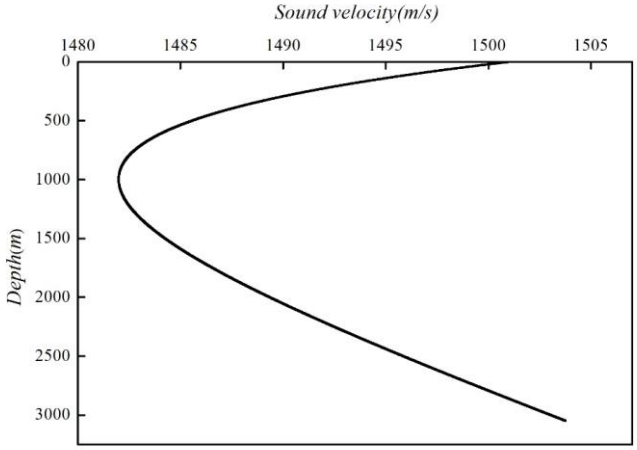

Figure 3. The background SVP obtained by the Munk standard equation.

Other simulation parameters are set as

- Water depth 3000 meters

Preprints (www.preprints.org) | NOT PEER-REVIEWED | Posted: 28 April 2023 doi:10.20944/preprints202304.1156.v1

- Draught of the transducer 1 meter
- Thickness of the unit water layer 1 meter
- Swath coverage of the MBS 120 degrees

In addition, we assumed that the seafloor topography is flat without fluctuation. To make the simulation more convincing, four types of sound velocity error were designed and shown as follows

1. The random error with variance is 2m/s;
2. The systematic error whose value is the constant and set as -1m/s;
3. The systematic error whose value increases with depth;
4. Including all the above terms.

Figure 4 shows the distribution of the four types of sound velocity errors.

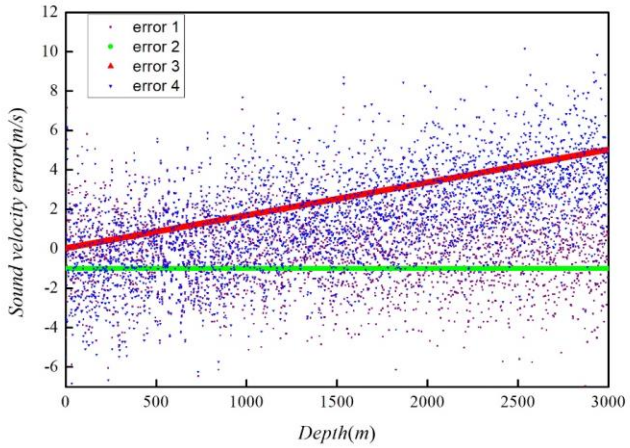

Figure 4. the distribution diagram of four types of error terms.

The propagation time observations are calculated by the CGRT[18]. Four types of sound velocity error were separately added to the background SVP. Then, calculate the positions of the beam footprint with the range of initial incidence angle from -60° to 60°. The result is shown in figure 5.

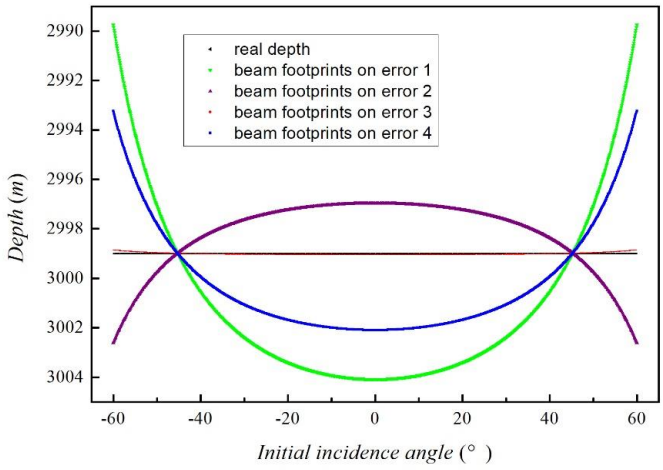

Figure 5. the beam footprints line on the different types of sound velocity error.

Figure 5 shows that it seems like the beam footprint lines on the different sound velocity errors would intersect with the real water depth at the same point when the initial incidence angle is about 45°. The beam footprint line on the error term 2 is the purple curve and its SVP area

Preprints (www.preprints.org) | NOT PEER-REVIEWED | Posted: 28 April 2023 doi:10.20944/preprints202304.1156.v1

difference is -2.9985×10^{-3}. The sounding of the central beam is smaller than the real water depth and the shape of the beam footprint line is convex shape. The SVP area difference of terms 1, 3, and 4 are 7.5×10^{3}, 27.723, and 4.5292×10^{3}, respectively. As shown in the green, red, and blue curves in figure 5. The soundings of the central beam are greater than the real water depth and the shape of the beam footprint line is concave. The larger the SVP area difference is, the more serious topography distortion happens. It indicates that the main factor that determines the seafloor topography distortion is the SVP area difference. The results are consistent with the theoretical analysis.

3.1. Application

The main factor that affects the seafloor topography distortion is the SVP area difference according to the previous analysis and simulation. In this section, a correction method was proposed to correct the topography distortion by compensating the SVP area. The specific steps of method are given below.

1. The shape of the beam footprint line is used to judge the positive or negative of the SVP area difference, which is obtained by the ray tracing method with measured SVP and propagation time observations.

2. An initial sound velocity correction δc and a given tolerance ε_D were set. The average depth D_m of the marginal beam on both sides was calculated. Then, calculate the depth difference D between the average depth D_m and the depth of the central beam. The sound velocity of each layer was added by the correction δc when D is bigger than zero. The sound velocity of each layer was reduced by the correction δc when D is smaller than zero. The SVP was updated in this way.

3. The depth difference D was recalculated by the updated SVP and marked as D_1. The difference between D and D_1 was calculated and marked as δ_D. If δ_D is less than the ε_D, jump out of the cycle and output the result. If δ_D is bigger than the ε_D, update the sound velocity correction value according to the following equation

$$\delta c = \delta c \cdot D_1 / \left(D - D_1 \right) \tag{19}$$

4. Return to step (2) and circularly calculated step (3) until δ_D is smaller than ε_D.

Another simulation was designed to correct the topography distortion caused by the four types of sound velocity error shown in figure 5. The initial sound velocity correction value δc is set as 1 m/s, and the given tolerance ε_D is 0.01 m.

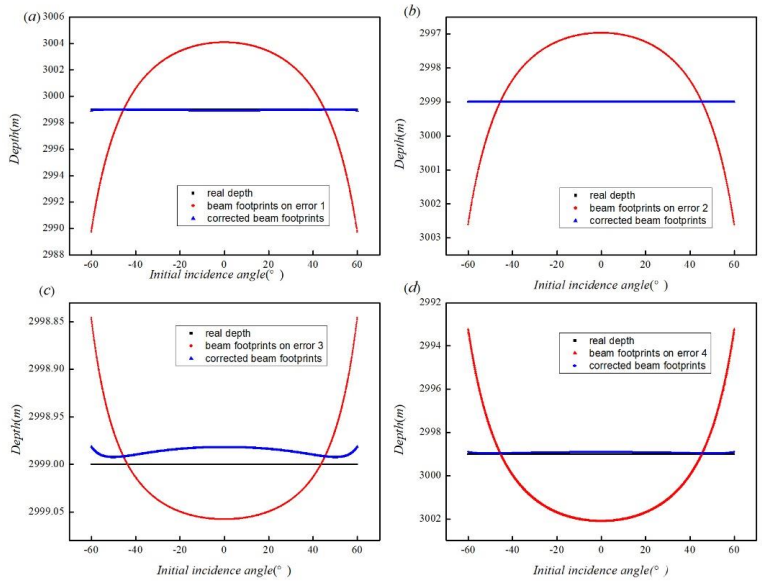

Figure 6. four beam footprint lines after being corrected.

Figure 6 shows the distorted topography after being corrected by this method. Both the beam footprint of the marginal beam and the central beam are close to the real water depth, and the

 doi:10.20944/preprints202304.1156.v1

magnitude of difference between them is only a few centimeters. It shows that the topography correction method can effectively improve the accuracy of the MBS soundings. Whether it is a system error, a random error, or both included. It proves the robustness of this method.

4. Conclusions

This study focuses on the problem of seafloor topography distortion caused by sound velocity error. We carried out a series of theoretical analyses about how the SVP area difference affects the topography distortion. An important fact that the sound velocity error has the least influence on MBS soundings when the initial incidence angle is about 45° was found. All the viewpoints have been verified by the two simulations. Finally, the following conclusions are drawn out.

1. The SVP area difference is the main factor that determines the position of the beam footprint of the central beam and the distortion extent of seafloor topography.

2. The beam footprint line and the real water depth will intersect when the initial incidence angle is about 45°. This conclusion is not affected by the various sound velocity errors.

3. Since the seafloor topography distortion mainly depends on the SVP area difference, we can add a correction of sound velocity to each layer for reducing the SVP area difference. This method can effectively improve the accuracy of MBS soundings.

Author Contributions: "Conceptualization, W.Z.S.; methodology, W.Z.S. and A.M.Z.; software, X.Z.; validation, W.Z.S. and X.Z.; formal analysis, W.Z.S.; investigation, Z.X.; resources, A.M.Z.; data curation, X.Z.; writing—original draft preparation, W.Z.S.; writing—review and editing, A.M.Z. and Z.X.; supervision,A.M.Z.; project administration, A.M.Z.; funding acquisition, A.M.Z.

Funding: This work is supported by China Postdoctoral Science Foundation (2022M723888) ; National Natural Science Foundation of China (Grant No. 41931076); National Key Research and Development Program of China (Grant No.2020YFB0505801); Financially supported by Laoshan Laboratory (LSKJ.202205101) .

References

1. Zhang, L., S. Ye, S. D. Zhou, F. Liu, and Y. Q. Han. Review of measurement techniques for temperature, salinity and depth profile of sea water, *Marine Science Bulletin*. 2017, 36(5): 481-489.
2. Petitt, R. A., R. W. Schmitt, and N. Brown. A new conductive-temperature-depth device for high resolution oceanographic measurement. *Oceans*. 2005, 2: 1070-1074.
3. Sun, W. C., J. Y. BAO, S. h. JIN, F. M. Xiao, and Y. Cui. Inversion of Sound Velocity Profiles by Correcting the Terrain Distortion. *Geomatics and information Science of Wuhan University*. 2016, 41(3): 349-355.
4. Canepa G., O. Bergem, and N. G. Pace. A New Algorithm for Automatic Processing of Bathmetric Data. *IEEE Journal of oceanic Engineering*. 2003, 28(1): 62-77.
5. Yang, F. l., J. B. Li, Z. Y. Wu, X. L. Jin, and F. Y. Chu. Fine Processing of Shallow Water Multi-beam Survey Data. *Acta Geodaetica et Cartographica Sinica.* 2008, 37(4): 444-457.
6. Zhu, Qing., and D. R. Li. Error Analysis and Processing of Multibeam Soundings. *Journal of Wuhan Technique University of Surveying and Mapping*. 1998, 23(1):1-4.
7. Xiao, Y. B., R. C. Peng, J. Y. Bao, J. Dong, and C. lv. Sounding Velocity Integrated Error Correction Method of Muti-beam Data Based on Kalman filtering. *Geomatics and information Science of Wuhan University.* 2020, 45(9): 1461-1468.
8. Zhao, J. H., H. M. Zhang, and J. Yan. Weakening Influence of Residual Error for MBS Sounding. *Geomatics and information Science of Wuhan University.* 2013, 38(10): 1184-1187.
9. Wu, Z. Y., X. L. Jin, Y. L. Zheng, J. B. Li, and P. Yu. Integrated error correction of multi-beam marginal sounding beam. *Acta Oceanologica Sinica.* 2005, 27(4): 88-94.
10. Yang, F. L., X. S. Lu, J. B. LI, L. T. Han and Z. Y. Zheng. Precise positioning of underwater static objects without sound speed profile *Marine Geodesy.* 2011, 34(2): 138-151.
11. Chadwell, C. D., and A. D. Sweeney. Acoustic ray-trace equations for seafloor geodesy. *Marine Geodesy.* 2010, 33(2-3): 164-184.
12. Sakic, Pi., V. Ballu, C. Wayne, and W. Guy. Acoustic Ray Tracing Comparisons in the Context of Geodetic Precise off-shore Positioning Experiments. *Marine Geodesy*. 2018, 41(4), 315–330.
13. Zhao, J. H., and J. N. Liu. Development of Method in Precise Multibeam Acoustic Bathymetry. *Geomatics and Information Science of Wuhan University.* 2002, 27(5): 453-457.
14. Sun, W. Z., X. D. Yin, A. M. Zeng, and Q. Liu.. Calculating the Starting Incidence Angle by Iterative Method for Positioning Seafloor Control Ponits. *Geomatics and Information Science of Wuhan University.* 2020, 45(10): 1588-1593.
15. Sun, W. Z., X. D. Yin, and A. M. Zeng. The Relationship between Propagation Time and Sound Velocity for Positioning Seafloor Reference Points. *Marine Geodesy.* 2019, 42(2): 186-200.
16. Geng, X. Y., Zielinski A. Precise Multibeam Acoustic Bathymetry. *Marine Geodesy.* 1999, 22: 157-167.
17. Munk, W. H. Sound channel in an exponentially stratified, with application to SOFAR. *The Journal of the Acoustical Society of America.* 1974, 55(2): 220-226.
18. Lu, X. P., S. F. Bian, M. T. Huang, and G. J. Zhai. An Improved Method for Calculating Average Sound Speed in Constant Gradient Sound Ray Tracing Technology. *Geomatics and Information Science of Wuhan University*. 2012, 37(5): 590-593.